Analytical Strip Method for Thin Isotropic Cylindrical Shells

*J. Taylor Perkins[1], Issam E. Harik[2]
[1]Ph.D Candidate, Department of Civil Engineering, University of Kentucky, USA
[2]Department of Civil Engineering, University of Kentucky, USA
Corresponding Author: J. Taylor Perkins

Abstract: *The Analytical Strip Method (ASM) for the analysis of thin isotropic cylindrical shells is presented in this paper. The system of three governing differential equations for the cylindrical shell are reduced to a single eighth order partial differential equation (PDE) in terms of a potential function. The PDE is solved as a single series form of the potential function, from which the displacement and force quantities are determined. The solution method applies to cylindrical shells with simply supported edges, clamped edges, free edges, or edges supported by isotropic beams. The cylindrical shell can be stiffened with isotropic beams in the circumferential direction placed anywhere along the length of the cylinder. Any combination of point loads, uniform loads, hydrostatic loads, patch loads, and line loads applied in the radial direction, can be incorporated in the solution. The results of the ASM are compared to results from existing analytical solutions and numerical solutions for several examples; the results for each of the methods were in good agreement. The ASM overcomes limitations of existing analytical solutions and provides an alternative to approximate numerical and semi-numerical methods.*

Keywords: *Analytical modeling, Thin shells, Stiffeners, Distributed loads, Line loads, Point loads*


I.   Introduction

Cylindrical Shells are important structural elements with widespread applications in various fields such as civil, environmental, mechanical, and aerospace engineering. Much effort has been dedicated to understanding the behavior of these structures. Several shell theories have been developed to simplify complex three-dimensional elasticity based solutions. These theories are roughly divided into two categories, thin shell theories which adopt Love's assumptions and higher order shell theories that relax one or more of the Love's assumptions (Kraus [1]). Due to the complexity of the governing equations for cylindrical shells, many of the existing analytical solutions are based on thin shell theory. Leissa [2] provides an excellent review of available thin shell theories.

Analytical solutions to cylindrical shells subjected to axisymmetric loads are widely available. Timoshenko and Woinowsky-Krieger [3] provide solutions for cylindrical shells with uniform internal pressure as well as cylindrical tanks subjected to hydrostatic loads. Due to the introduction of a second variable in the circumferential direction, non-axisymmetric type loadings are difficult to incorporate in the solution. Bijlaard [4] developed a double series solution for cylindrical shells subjected to a patch load as well as a similar solution for point loads. Odqvist [5], Hoff et al. [6], Cooper [7], and Naghdi [8] have developed unique solutions for cylindrical shells subjected to a uniform line load along a generator. Meck [9] presented a solution for line loads applied along the circumferential direction.

The objective of this paper is to develop an analytical strip method (ASM) of solution for stiffened isotropic thin cylindrical shells. The ASM was first developed by Harik and Salamoun ([10], [11]) for the analysis of thin orthotropic and stiffened rectangular plates subjected to uniform, partial uniform, patch, line, partial line, and point loads or any combination thereof. The solution procedure requires that the structure be divided into strips based on the geometric discontinuities and load patterns applied (Fig. 1). The governing differential equation for each strip is solved analytically and the applicable continuity and boundary conditions are used to combine the solutions for the strips.

The primary contribution of the ASM is in its ability to handle a wide variety of loading and geometric configurations. At present, analytical solutions are limited to axisymmetric and simple non-axisymmetric loadings applied to cylindrical shells of basic geometry. Other more complex cases must utilize numerical or semi-numerical techniques. Unlike numerical based solutions, the accuracy of the ASM does not depend on the number of strips within the structure, but rather the number of modes considered in the series solution.
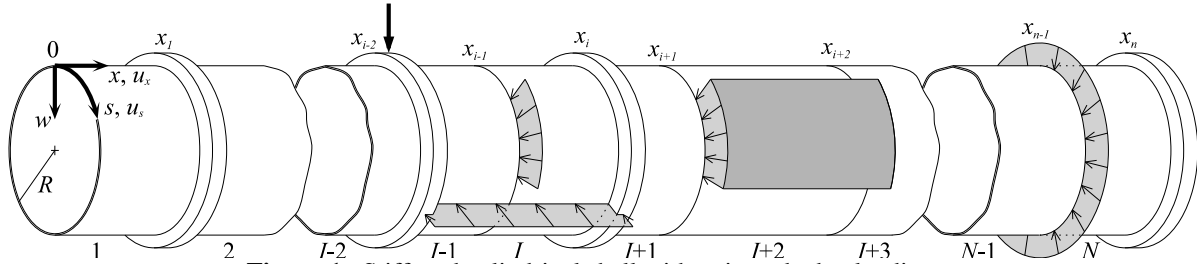
Figure 1. Stiffened cylindrical shell with strip and edge loadings
Note: The stiffeners are concentric with the shell

II. Governing Differential Equation

The surface coordinate system used in the derivation of the governing equation for a cylindrical strip is shown in Fig. 1. The strain-displacement equations associated with thin shell theory are given as (Kraus [1]):

$$\epsilon_x = \frac{\partial u_x}{\partial x}, \qquad \epsilon_s = \frac{\partial u_s}{\partial s} + \frac{w}{R}, \qquad \gamma_{xs} = \frac{\partial u_s}{\partial x} + \frac{\partial u_x}{\partial s} \tag{1a, b, c}$$

$$\kappa_x = -\frac{\partial^2 w}{\partial x^2}, \quad \kappa_s = \frac{\partial}{\partial s}\left(\frac{u_s}{R} - \frac{\partial w}{\partial s}\right), \quad \kappa_{xs} = \frac{1}{R}\frac{\partial u_s}{\partial x} - 2\frac{\partial^2 w}{\partial x \partial s} \tag{1d, e, f}$$

And the equilibrium equations are (Kraus [1]):

$$\frac{\partial N_x}{\partial x} + \frac{\partial N_{sx}}{\partial s} + q_x = 0 \tag{2a}$$

$$\frac{\partial N_{xs}}{\partial x} + \frac{\partial N_s}{\partial s} + \frac{Q_s}{R} + q_s = 0 \tag{2b}$$

$$\frac{\partial Q_x}{\partial x} + \frac{\partial Q_s}{\partial s} - \frac{N_s}{R} + q = 0 \tag{2c}$$

$$\frac{\partial M_x}{\partial x} + \frac{\partial M_{xs}}{\partial s} - Q_x = 0 \tag{2d}$$

$$\frac{\partial M_{xs}}{\partial x} + \frac{\partial M_s}{\partial s} - Q_s = 0 \tag{2e}$$

The five equilibrium equations are reduced to three by substituting (2d) and (2e) into (2c). Substitution of the strain-displacement equations into the equilibrium equations yield a system of three differential equations that may be presented as:

$$\begin{bmatrix} L_{11} & L_{12} & L_{13} \\ L_{12} & L_{22} & L_{23} \\ L_{13} & L_{23} & L_{33} \end{bmatrix} \begin{Bmatrix} u_x \\ u_s \\ w \end{Bmatrix} = \begin{Bmatrix} q_x \\ q_s \\ q \end{Bmatrix} \tag{3}$$

where L_{ij} are differential operators:

$$L_{11} = A\frac{\partial^2}{\partial x^2} + \frac{1-\nu}{2}A\frac{\partial^2}{\partial s^2} \tag{4a}$$

$$L_{12} = \frac{1+\nu}{2}A\frac{\partial^2}{\partial x \partial s} \tag{4b}$$

$$L_{13} = \frac{\nu}{R}A\frac{\partial}{\partial x} \tag{4c}$$

$$L_{22} = \left(\frac{1-\nu}{2}A + \frac{1-\nu}{2R^2}D\right)\frac{\partial^2}{\partial x^2} + (A + D)\frac{\partial^2}{\partial s^2} \tag{4d}$$

$$L_{23} = \frac{1}{R}A\frac{\partial}{\partial s} - \frac{1}{R}D\frac{\partial^3}{\partial x^2 \partial s} - \frac{1}{R}D\frac{\partial^3}{\partial s^3} \tag{4e}$$

$$L_{33} = \frac{1}{R^2}A + D\frac{\partial^4}{\partial x^4} + 2D\frac{\partial^4}{\partial x^2 \partial s^2} + D\frac{\partial^4}{\partial s^4} \tag{4f}$$

A and D are the extensional and bending stiffness of the shell:

$$A = \frac{Et}{1-v^2} \tag{5a}$$

$$D = \frac{Et^3}{12(1-v^2)} \tag{5b}$$

And *t* is the thickness, *E* is the elastic modulus, and *v* is Poisson's ratio.

The displacements in the *x*, *s*, and *r* direction, u_x, u_s, and *w*, can be presented in terms of the potential function $\Phi(x,s)$ (Sharma et al. [12]):

$$u_x = (L_{12}L_{23} - L_{13}L_{22})\Phi(x,s) \tag{6a}$$

$$u_s = (L_{13}L_{21} - L_{23}L_{11})\Phi(x,s) \tag{6b}$$

$$w = (L_{11}L_{22} - L_{12}L_{21})\Phi(x,s) \tag{6c}$$

For the case of radial loads only, the three equations can be combined into a single eighth order differential equation expressed in terms of the potential function Φ (Sharma et al. [12]):

$$F_{80}\frac{\partial^8\Phi}{\partial x^8} + F_{62}\frac{\partial^8\Phi}{\partial x^6\partial s^2} + F_{44}\frac{\partial^8\Phi}{\partial x^4\partial s^4} + F_{26}\frac{\partial^8\Phi}{\partial x^2\partial s^6} + F_{08}\frac{\partial^8\Phi}{\partial s^8} + F_{42}\frac{\partial^6\Phi}{\partial x^4\partial s^2} + F_{24}\frac{\partial^6\Phi}{\partial x^2\partial s^4} + F_{06}\frac{\partial^6\Phi}{\partial s^6} + F_{40}\frac{\partial^4\Phi}{\partial x^4} +$$
$$F_{22}\frac{\partial^4\Phi}{\partial x^2\partial s^2} + F_{04}\frac{\partial^4\Phi}{\partial s^4} = q(x,s) \tag{7}$$

The coefficients F_{ij} are:

$$F_{80} = \frac{1-v}{2R^2}AD^2 + \frac{1-v}{2}A^2D \tag{8a}$$

$$F_{62} = \frac{(v-1)(v-5)}{4R^2}AD^2 + 2(1-v)A^2D \tag{8b}$$

$$F_{44} = \frac{(v-1)(v+3)}{2R^2}AD^2 + 3(1-v)A^2D \tag{8c}$$

$$F_{26} = \frac{(1-v)^2}{4R^2}AD^2 + 2(1-v)A^2D \tag{8d}$$

$$F_{08} = \frac{1-v}{2}A^2D \tag{8e}$$

$$F_{42} = \frac{(1-v)(v+2)}{R^2}A^2D \tag{8f}$$

$$F_{24} = \frac{(1-v)(v+3)}{R^2}A^2D \tag{8g}$$

$$F_{06} = \frac{(1-v)}{R^2}A^2D \tag{8h}$$

$$F_{40} = \frac{(v-1)^2(v+1)}{2R^4}A^2D + \frac{(v-1)^2(v+1)}{2R^2}A^3 \tag{8i}$$

$$F_{22} = \frac{(1-v)(3v+5)}{4R^4}A^2D \tag{8j}$$

$$F_{04} = \frac{(1-v)}{2R^4}A^2D \tag{8k}$$

Where *A* and *D* are the extensional and bending stiffness provided in (5a) and (5b).

III. Isotropic Beam Equations

The following differential equations can be derived from the equilibrium of an isotropic curved beam element (Vlasov [13]):

$$q_{xb} = E_bI_r\left(\frac{d^4u_{xb}}{ds^4} - \frac{1}{R}\frac{d^2\phi_b}{ds^2}\right) + \frac{E_bC_w}{R}\left(\frac{d^4\phi_b}{ds^4} + \frac{1}{R}\frac{d^4u_{xb}}{ds^4}\right) - \frac{G_bJ_b}{R}\left(\frac{d^2\phi_b}{ds^2} + \frac{1}{R}\frac{d^2u_{xb}}{ds^2}\right) \tag{9}$$

$$q_{rb} = E_b I_x \left(\frac{d^4 w_b}{ds^4} - \frac{1}{R} \frac{d^3 u_{sb}}{ds^3} \right) + \frac{E_b A_b}{R} \left(\frac{du_{sb}}{ds} + \frac{1}{R} w_b \right) \tag{10}$$

$$q_{sb} = \frac{E_b I_x}{R} \left(\frac{d^3 w_b}{ds^3} - \frac{1}{R} \frac{d^2 u_{sb}}{ds^2} \right) - E_b A_b \left(\frac{d^2 u_{sb}}{ds^2} + \frac{1}{R} \frac{dw_b}{ds} \right) \tag{11}$$

$$m_{xb} = \frac{E_b I_r}{R} \left(-\frac{d^2 u_{xb}}{ds^2} + \frac{1}{R} \phi_b \right) + E_b C_w \left(\frac{d^4 \phi_b}{ds^4} + \frac{1}{R} \frac{d^4 u_{xb}}{ds^4} \right) - G_b J_b \left(\frac{d^2 \phi_b}{ds^2} + \frac{1}{R} \frac{d^2 u_{xb}}{ds^2} \right) \tag{12}$$

The terms q_{xb}, q_{rb}, and q_{sb} are the distributed forces per unit length applied to the beam in the x, r, and s directions (Fig. 2); m_{xb} is the twisting moment per unit length applied to the beam; u_{xb}, u_{sb}, and w_b are the deflections of the beam in the x, r, and s directions (Fig. 2); ϕ_b is the twist angle of the beam; R is the radius measured to the centroid of the beam; $E_b I_r$ = flexural rigidity about the r-axis (Fig. 2); $E_b I_x$ = flexural rigidity about the x-axis (Fig. 2); $E_b A_b$ = axial stiffness of the beam; $G_b J_b$ = torsional rigidity of the beam; $E_b C_w$ = warping rigidity of the beam.
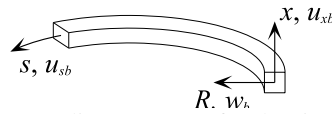

Figure 2. Coordinate system for the ring stiffener

IV. Analytical Strip Method

4.1 General Solution

The solution of the differential equation for a general strip assumes that the form for the potential function Φ satisfies continuity at the surface coordinate $s = 0$ and $s = 2\pi R$. Let:

$$\Phi = \sum_n^\infty \phi_n(x) \cos(\beta_n s) \tag{13}$$

Where:

$$\beta_n = \frac{n}{R} \tag{14}$$

Substituting (13) into the governing differential equation [(7)], multiplying both sides of the equation by $\cos(\beta_m s)$, integrating from $s = 0$ to $s = 2\pi R$, and summing from $m = 0$ to $m = \infty$ yields the following equation by orthogonality:

$$\sum_m^\infty \left\{ F_{8m}^* \frac{d^8 \phi_m(x)}{dx^8} + F_{6m}^* \frac{d^6 \phi_m(x)}{dx^6} + F_{4m}^* \frac{d^4 \phi_m(x)}{dx^4} + F_{2m}^* \frac{d^2 \phi_m(x)}{dx^2} + F_{0m}^* \phi_m(x) \right\} = \frac{1}{2\pi R} \int_0^{2\pi R} q(x,s) ds +$$

$$m{=}1\infty 1\pi R 02\pi R q(x,s)\cos\beta m s ds \tag{15}$$

Where:

$$F_{8m}^* = F_{80} \tag{16a}$$

$$F_{6m}^* = -F_{62} \beta_m^{\ 2} \tag{16b}$$

$$F_{4m}^* = F_{44} \beta_m^{\ 4} - F_{42} \beta_m^{\ 2} + F_{40} \tag{16c}$$

$$F_{2m}^* = -F_{26} \beta_m^{\ 6} + F_{24} \beta_m^{\ 4} - F_{22} \beta_m^{\ 2} \tag{16d}$$

$$F_{0m}^* = F_{08} \beta_m^{\ 8} - F_{06} \beta_m^{\ 6} + F_{04} \beta_m^{\ 4} \tag{16e}$$

For $m = 0$, $F_{20}^* = F_{00}^* = 0$ and for $m = 1$, $F_{01}^* = 0$.

(15) is an infinite set of linear 8th order ordinary differential equations for $\phi_m(x)$ ($m = 0, 1, 2, \dots, \infty$). The solution is obtained by superposition of the associated homogeneous and particular solutions:

$$\Phi(x, s) = \Phi_H(x, s) + \Phi_P(x, s) \tag{17}$$

where the homogeneous solution:

$$\Phi_H(x,s) = \sum_m^\infty \phi_{Hm}(x) \cos(\beta_m s) \tag{18}$$

and the particular solution:

$$\Phi_P(x,s) = \sum_m^\infty \phi_{Pm}(x) \cos(\beta_m s) \tag{19}$$

4.2 Homogeneous Solution
The homogeneous solution for mode m, $\phi_{Hm}(x)$, is expressed as:

$$\phi_{Hm}(x) = e^{\gamma_m \beta_m x} \tag{20}$$

The characteristic equation of (20) for mode $m = 0$ is:

$$F_8^* \gamma_m{}^8 + F_6^* \gamma_m{}^6 + F_4^* \gamma_m{}^4 = 0 \tag{21}$$

And the homogeneous solution for mode $m = 0$ is:

$$\Phi_{H0}(x,s) =$$
$$C_{10} + C_{20}x + C_{30}x^2 + C_{40}x^3 + [C_{50}\cosh(\gamma_{30}x) + C_{60}\sinh(\gamma_{30}x)]\cos(\gamma_{40}x) + [C_{70}\cosh(\gamma_{30}x) +$$
$$C80\sinh(\gamma30x)\sin(\gamma40x) \tag{22}$$

The characteristic equation of (20) for mode $m = 1$ is:

$$F_8^* \gamma_m{}^8 + F_6^* \gamma_m{}^6 + F_4^* \gamma_m{}^4 + F_2^* \gamma_m{}^2 = 0 \tag{23}$$

And the homogeneous solution for mode $m = 1$ is:

$$\Phi_{H1}(x,s) = \left\{ \begin{array}{c} C_{11} + C_{21}x + C_{31}e^{\gamma_{31}x} + C_{41}e^{-\gamma_{31}x} \\ +[C_{51}\cosh(\gamma_{11}x) + C_{61}\sinh(\gamma_{11}x)]\cos(\gamma_{21}x) \\ +[C_{71}\cosh(\gamma_{11}x) + C_{81}\sinh(\gamma_{11}x)]\sin(\gamma_{21}x) \end{array} \right\} \cos(\beta_1 s) \tag{24}$$

The characteristic equation of (20) for all other modes ($m = 2, 3, …,\infty$) is:

$$F_8^* \gamma_m{}^8 + F_6^* \gamma_m{}^6 + F_4^* \gamma_m{}^4 + F_2^* \gamma_m{}^2 + F_0^* = 0 \tag{25}$$

And the homogeneous solution for all other modes ($m = 2, 3, …, \infty$) is:

$$\Phi_{Hm}(x,s) = \left\{ \begin{array}{c} [C_{1m}\cosh(\gamma_{1m}x) + C_{2m}\sinh(\gamma_{2m}x)]\cos(\gamma_{2m}x) \\ +[C_{3m}\cosh(\gamma_{1m}x) + C_{4m}\sinh(\gamma_{1m}x)]\sin(\gamma_{2m}x) \\ +[C_{5m}\cosh(\gamma_{3m}x) + C_{6m}\sinh(\gamma_{3m}x)]\cos(\gamma_{4m}x) \\ +[C_{7m}\cosh(\gamma_{3m}x) + C_{8m}\sinh(\gamma_{3m}x)]\sin(\gamma_{4m}x) \end{array} \right\} \cos(\beta_m s) \tag{26}$$

(21), (23), and (25) can be reduced to quartic equations for which the characteristic roots can be solved analytically (Editing Group of the Manual of Mathematics [14]). The constants C_{dm} ($d = 1,2,...,8$) for each mode ($m = 1,2,...,\infty$) are determined by the boundary conditions at $x = 0$ and $x = x_n$ and the continuity conditions at $x = x_i$ ($i = 1,2,...,n-1$), see Fig. 1.

4.3 Particular Solution
The particular solution is dependent upon the load distribution applied to the strip. For a given strip loading, the load distribution function, $q(x,s)$, is expressed as:

$$q(x,s) = q_0 f(x) g(s) \tag{27}$$

where q_0 is the load amplitude and $f(x)$ and $g(s)$ are the load distribution functions in the *x* and *s* directions. Substituting into the right hand side of (15) yields, for mode $m = 0$:

$$\frac{q_0 f(x)}{2\pi R} \int_0^{2\pi R} g(s)ds \tag{28}$$

And for all other modes ($m = 1, 2, …, \infty$):

$$\frac{q_0 f(x)}{\pi R} \int_0^{2\pi R} g(s) \cos(\beta_m s)\, ds \tag{29}$$

The potential function, $\phi_{pm}(x)$, can be found for a wide range of commonly encountered load distributions. The particular solution for most common strip loadings are shown in Table 1. When a strip is subjected to more than one load, the method of superposition is employed to determine the particular solution.

4.4 Edge Loading

For cylinders subjected to point loads and radial line loads distributed along the circumferential direction, the structure is divided into strips such that the loads coincide with the edges of the strips (Fig. 1). These loads are expressed as a Fourier series and incorporated into the solution as shear force discontinuities between strips. Table 2 presents the edge loading function $\psi_i(s)$ for several common loadings.

When an edge is subjected to a combination of loads, the method of superposition is employed to determine the edge loading function.

4.5 Boundary Conditions

The boundary conditions along the edges $x = 0$ and $x = x_n$ are:

For simply supported edges: $u_x = 0, \quad u_s = 0, \quad w = 0, \quad M_x = 0$ (30a, b, c, d)

For clamped edges: $u_x = 0, \quad u_s = 0, \quad w = 0, \quad \frac{\partial w}{\partial x} = 0,$ (31a, b, c, d)

For free edges: $Q_x = \psi, \quad N_x = 0, \quad N_{xs} = 0, \quad M_x = 0,$ (32a, b, c, d)

For beam support: $w = w_b, \quad \frac{dw}{dx} = \phi_b, \quad Q_x = q_{rb} + \psi, \quad M_x = m_{tb}$ (33a, b, c, d)

4.6 Continuity Conditions

The following continuity conditions are applied along the edge between strips I and $I + 1$ at $x = x_i$:

$$u_{xI} = u_{x(I+1)}, \quad u_{sI} = U_{s(I+1)}, \quad w_I = w_{(I+1)}, \quad \frac{\partial w_I}{\partial x} = \frac{\partial w_{(I+1)}}{\partial x} \tag{34a, b, c, d}$$

$$M_{xI} = M_{x(I+1)}, \quad N_{xI} = N_{x(I+1)}, \quad Q_{xI} = Q_{x(I+1)} + \psi_i, \quad N_{xsI} = N_{xs(I+1)} \tag{35a, b, c, d}$$

When a beam is present at $x = x_i$, the following continuity conditions are imposed along the common edge $x = x_i$, between strips I and $I+1$.

$$u_{xI} = u_{x(I+1)}, \quad u_{sI} = U_{s(I+1)}, \quad w_I = w_{(I+1)}, \quad \frac{\partial w_I}{\partial x} = \frac{\partial w_{(I+1)}}{\partial x} = \phi_b \tag{36a, b, c, d}$$

$$m_{tb} = M_{x(I+1)} - M_{xI}, \quad q_{xb} = N_{x(I+1)} - N_{xI}, \tag{37a, b}$$

$$q_{rb} = Q_{x(I+1)} - Q_{xI} + \psi_i, q_{sb} = N_{xs(I+1)} - N_{xsI} \tag{38c, d}$$

V. Solution

A cylindrical shell is divided into *N*-strips (Fig. 1) depending on the number of loading discontinuities and the locations of the ring stiffeners. For each of the *N*-strips, eight equations are generated from the boundary and continuity conditions. This yields a unique 8*N* system of equations for each mode ($m = 0, 1, 2, \ldots, \infty$). Solution of this system of equations provide the constants C_{dmI} ($d = 1, 2, \ldots, 8$) in the homogeneous solution. The potential function Φ_I for each strip I ($I = 1, 2, \ldots, N$) is derived by summing the homogeneous and particular solutions. The potential function is then back-substituted into the relevant force and displacement equations.

VI. Application

6.1 Computation of ASM Solutions

Because of the ill-conditioned nature of the solution, the ASM is susceptible to numerical instabilities when computing solutions using double precision floating point format. To eliminate this concern, examples are computed with a MATLAB program using an arbitrary-precision package.

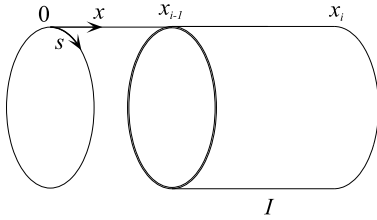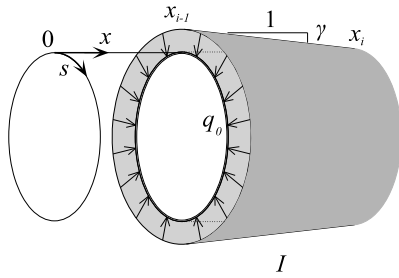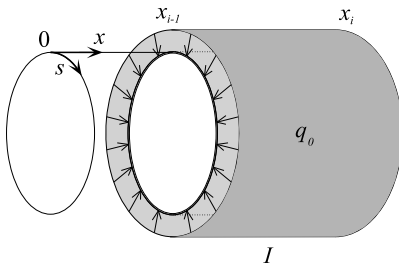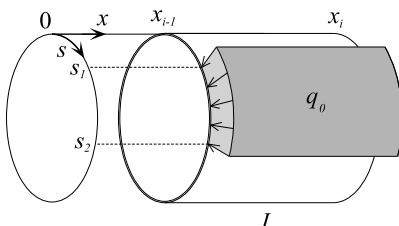**Table 1.** Particular solution $\Phi_{PI}(x,s)$ for cylindrical strip I
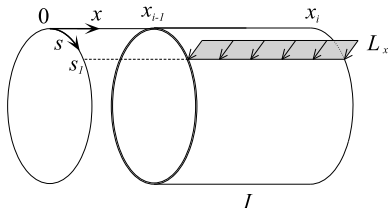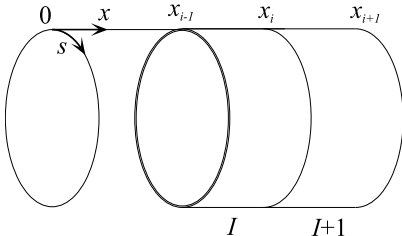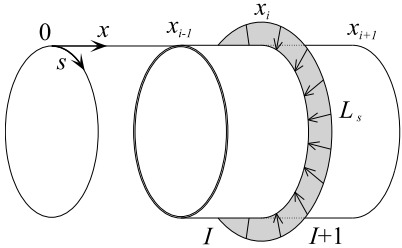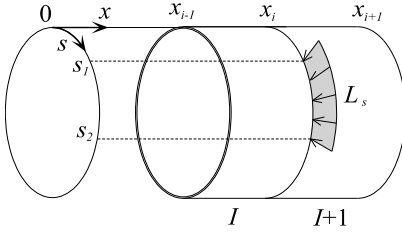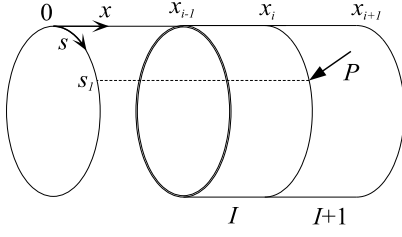
Load Case	$\Phi_{PI}(x,s)$
Case 1 - Zero load	

$$\Phi_{PI}(x,s) = 0$$

Case 2 - Linearly varying load (hydrostatic load)

$$q(x,s) = q_0 - \gamma(x - x_{i-1})$$

$$\Phi_{PIm=0}(x,s) = \frac{q_0}{24A_{40}^*}x^4 - \frac{\gamma}{120A_{40}^*}x^5$$

$$\Phi_{PIm=1,2,\ldots,\infty}(x,s) = 0$$

Case 3 - Uniform load q_0

$$\Phi_{PIm=0}(x,s) = \frac{q_0}{24A_{40}^*}x^4$$

$$\Phi_{PIm=1,2,\ldots,\infty}(x,s) = 0$$

Case 4 - Partial uniform load q_0

$$\Phi_{PIm=0}(x,s) = \frac{q_0}{48\pi RA_{40}^*}(s_2 - s_1)x^4$$

$$\Phi_{PIm=1}(x,s) = \frac{q_0}{2\pi RA_{21}^*}\left[\sin\left(\frac{s_2}{R}\right) - \sin\left(\frac{s_1}{R}\right)\right]x^2\cos\left(\frac{s}{R}\right)$$

$$\Phi_{PIm=2,3,\ldots,\infty}(x,s) = \frac{q_0}{m\pi RA_{0m}^*}\left[\sin\left(\frac{m}{R}s_2\right) - \sin\left(\frac{m}{R}s_1\right)\right]\cos\left(\frac{m}{R}s\right)$$

Case 5 - Line load L_x

$$\Phi_{PIm=0}(x,s) = \frac{L_x}{48\pi RA_{40}^*}x^4$$

$$\Phi_{PIm=1}(x,s) = \frac{L_x}{2\pi RA_{21}^*}\cos\left(\frac{s_1}{R}\right)x^2\cos\left(\frac{s}{R}\right)$$

$$\Phi_{PIm=2,3,\ldots,\infty}(x,s) = \frac{L_x}{\pi RA_{0m}^*}\cos\left(\frac{m}{R}s_1\right)\cos\left(\frac{m}{R}s\right)$$

Table 2. Edge loading function $\psi_i(s)$ along the edge $x = x_i$

Load Case	$\psi_i(s)$
Case 1 - Zero load	

$$\psi_i(s) = 0$$

Case 2 - Line load L_s in s direction

$$\psi_{im=0}(s) = L_s$$

$$\psi_{im=1,2,\dots,\infty}(s) = 0$$

Case 3 - Partial line load L_y

$$\psi_{im=0}(s) = \frac{L_s(s_2 - s_1)}{2\pi R}$$

$$\psi_{im=1,2,\dots,\infty}(s) = \frac{2L_s}{m\pi} \sin\left[\frac{m}{2R}(s_2 - s_1)\right] \cos\left[\frac{m}{R}\left(s - \frac{s_1 + s_2}{2}\right)\right]$$

Case 4 - Concentrated point load P

$$\psi_{im=0}(s) = \frac{P}{2\pi R}$$

$$\psi_{im=1,2,\dots,\infty}(s) = \frac{P}{\pi R} \cos\left[\frac{m}{R}(s - s_1)\right]$$

6.2 Example 1: Cylindrical Shell Subjected to Non-Axisymmetric Loads

The purpose of this example is to compare the Analytical Strip Method (ASM) results for cylindrical shells subjected to non-axisymmetric loads to an existing analytical solution developed by Bijlaard [4] for the design of pressure vessels subjected to point and patch loads.

The shells in Fig. 3 and Fig. 4 are simply supported at the ends, $(\partial ux/\partial x) = u_s = w = M_x = 0$, and are subject to a point load and a patch load at mid-length, respectively. The magnitude of the point load is designated as P, while the resultant (or total) magnitude of the patch load is $P^* = 4pc_1c_2$, where p is the

distributed load and c_1 and c_2 are the half-lengths of the patch area in the circumferential and longitudinal direction respectively (Fig. 4). Poisson's ratio $v = 0.30$.
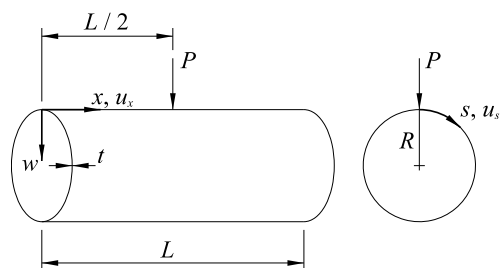
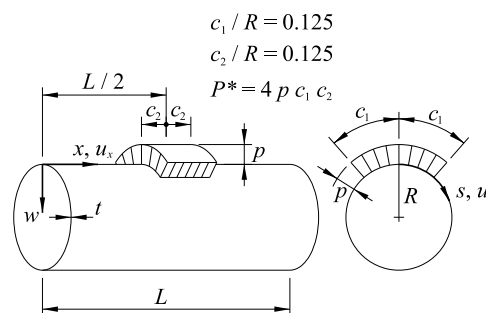**Figure 3.** Cylindrical Shell Subjected to Point Load   **Figure 4.** Cylindrical Shell Subjected to Patch Load

Table 3 presents the dimensionless radial deflection and force quantities corresponding to bending moments M_s and M_x as well as membrane forces N_s and N_x. The results are presented for prescribed radius-to-thickness ratios (R/t) and length-to-radius ratios (L/R) at $x = L/2$, $s = 0$. The results are presented for an existing analytical solution (Bijlaard [4]), the Analytical Strip Method (ASM), and a finite-element (FEM) solution generated using SAP2000.

The results show excellent agreement between the ASM and FEM solutions; the dimensionless quantities are all within 2% difference. There is also good agreement between the existing analytical solution (Bijlaard [4]) and the ASM for the dimensionless deflection quantities and the dimensionless force quantities corresponding to M_s and N_x; the values are predominately within 3% difference. The dimensionless force quantities for M_x and N_s show more variation between the existing analytical solution (Bijlaard [4]) and the ASM; the difference in the two solutions is as much as 10% with the larger differences occurring at larger radius-to-thickness ratios.

In development of the existing analytical solution, Bijlaard's intent was to develop a set of practical equations that could be used in practice for the evaluation of local stresses in pressure vessels. As a result, there were several simplifications made in his formulation at the cost of accuracy in the solution; the most significant being the neglect of the fourth-order terms in his combined eight-order differential equation. The neglected terms correspond to the absence of:

$$\frac{t^2}{12R^2}\left[(1-v)\frac{\partial^2 v}{\partial x^2} + \frac{\partial^2 v}{\partial s^2}\right] \tag{39}$$

in the second of Timoshenko's [3] three uncoupled differential equations. This term is fully incorporated into the ASM solution. The neglect of this term will not fully capture the membrane stiffness of the shell and is likely a major contributor in the differences in the dimensionless M_x and N_s values between the existing analytical solution (Bijlaard [4]) and the ASM and FEM.

The ASM results in Table 3 are based on summation of the first 51 modes. For the case of radius-to-thickness ratio of 100 and length-to-radius ratio of 3, Table 4 presents the cumulative dimensionless deflection and force quantities for selected modes. The solution demonstrates good convergence. The dimensionless force quantity associated with bending moments M_s and M_x converged slower than the other results with variation of 1.7% and 0.6%, respectively, between modes 40 and 50.

Table 3. Dimensionless deflection and forces at $x = L/2$ and $s = 0$ for the cylindrical shell subjected to point load, P, in Figure 3 and to patch load, $P^* = 4pc_1c_2$, with $c_1 = c_2$ in Figure 4.

R/t	L/R	Method	Point Load $\dfrac{wER}{P}$	Patch Load $\dfrac{wER}{P^*}$	$\dfrac{M_s}{P^*}$	$\dfrac{M_x}{P^*}$	$-\dfrac{N_sR}{P^*}$	$-\dfrac{N_xR}{P^*}$
15	3	Bijlaard[a]	300	272	0.1324	0.1057	2.613	2.320
		ASM[b]	296	267	0.1321	0.1045	2.482	2.282
		FEM[c]	299	269	0.1333	0.1052	2.460	2.300
	6	Bijlaard	468	442	0.1438	0.1100	2.592	2.640
		ASM	463	434	0.1438	0.1079	2.439	2.619
		FEM	469	438	0.1452	0.1086	2.420	2.640
	10	Bijlaard	601	576	0.1463	0.1102	2.574	2.784
		ASM	597	566	0.1473	0.1087	2.428	2.719
		FEM	586	570	0.1486	0.1095	2.420	2.740
50	3	Bijlaard	4352	3645	0.0863	0.0559	6.451	7.120
		ASM	4324	3573	0.0857	0.0556	6.367	7.038
		FEM	4350	3596	0.0864	0.0559	6.360	7.060
	8	Bijlaard	7631	6924	0.0967	0.0614	6.482	8.064
		ASM	7608	6826	0.0956	0.0585	6.310	8.001
		FEM	7656	6844	0.0964	0.0588	6.300	8.020
	20	Bijlaard	13430	12930	0.1030	0.0634	6.434	8.704
		ASM	12667	11853	0.1007	0.0599	6.292	8.466
		FEM	12702	11890	0.1015	0.0603	6.280	8.500
100	3	Bijlaard	20227	15800	0.0626	0.0343	9.578	12.784
		ASM	20256	15643	0.0617	0.0341	9.517	12.744
		FEM	20532	15660	0.0627	0.0344	9.520	12.760
	8	Bijlaard	34350	30136	0.0716	0.0394	9.792	14.192
		ASM	34747	29857	0.0704	0.0366	9.450	14.142
		FEM	35032	29870	0.0711	0.0368	9.460	14.160
	30	Bijlaard	74379	71448	0.0767	0.0400	9.618	15.472
		ASM	74124	68968	0.0760	0.0382	9.432	15.400
		FEM	74472	69020	0.0767	0.0385	9.440	15.420
300	3	Bijlaard	231738	158362	0.0337	0.0137	13.696	29.328
		ASM	234848	157615	0.0332	0.0135	13.617	29.188
		FEM	237974	157180	0.0337	0.0136	13.620	29.140
	8	Bijlaard	402590	313842	0.0406	0.0172	14.963	32.288
		ASM	397532	315039	0.0394	0.0154	13.532	32.197
		FEM	404260	314592	0.0399	0.0155	13.540	32.160
	20	Bijlaard	625855	566530	0.0440	0.0180	14.584	33.424
		ASM	676570	590498	0.0431	0.0165	13.512	34.344
		FEM	683356	590092	0.0436	0.0166	13.520	34.300
	40	Bijlaard	968910	925438	0.0453	0.0180	14.200	34.128
		ASM	1014420	925796	0.0453	0.0171	13.504	35.043
		FEM	1021380	925506	0.0458	0.0172	13.520	35.000

[a]Bijlaard = Existing Analytical Solution (Bijlaard [4])
[b] ASM = Analytical Strip Method
[c] FEM = Finite Element Solution (SAP2000)

Table 4. ASM cumulative dimensionless deflections and forces at $x = L/2$ and $s = 0$ for the shell subjected to a point load, P, in Fig. 3 and to a patch load, $P^* = 4pc_1c_2$ with $c_1 = c_2$ in Fig.4; $R/t = 100$ and $L/R = 3$.
Note: $w = \sum_0^m w_m$, $M = \sum_0^m M_m$, $N = \sum_0^m N_m$

Mode	Point Load	Patch Load				
m	$\dfrac{wER}{P}$	$\dfrac{wER}{P^*}$	$\dfrac{M_s}{P^*}$	$\dfrac{M_x}{P^*}$	$-\dfrac{N_sR}{P^*}$	$-\dfrac{N_xR}{P^*}$
0	102	64	0.0001	0.0004	0.641	0.000
1	371	255	0.0004	0.0012	1.917	0.227
2	1043	842	0.0008	0.0021	3.174	1.127
5	9930	9054	0.0146	0.0098	6.410	7.212
10	16698	14448	0.0435	0.0248	8.972	11.530
20	19401	15648	0.0644	0.0348	9.510	12.738
30	19969	15666	0.0647	0.0350	9.514	12.752
40	20167	15643	0.0627	0.0343	9.516	12.744
50	20256	15643	0.0617	0.0341	9.517	12.744

6.3 Example 2: Cylindrical Shell Subjected to Line Load along the Generator

The purpose of this example is to compare the Analytical Strip Method (ASM) results for a cylindrical shell subjected to a line load with an existing analytical solution developed by Hoff et al. [6] with numerical results derived by Kempner [15].

The shell in Fig. 5 is simply supported at the ends, $(^{\partial ux}/_{\partial x}) = u_s = w = M_x = 0$, and is subject to a line load centered at mid-length of the cylinder. The line load has a total magnitude designated as $P^* = 2c_2p$ and a half-length designated at c_2. The modulus of elasticity $E = 2.07\text{x}10^8\text{kPa}$ ($30\text{x}10^6$ psi) and Poisson's ratio $v = 0.30$.
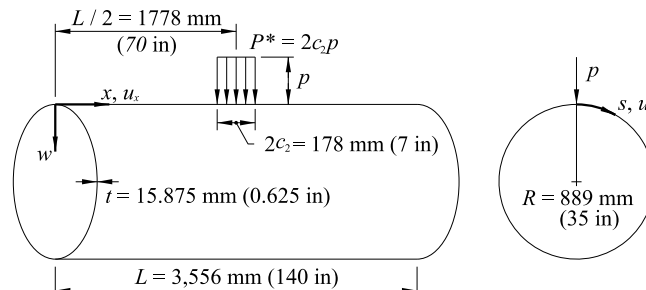

Figure 5. Cylindrical shell subjected to a line load

Table 5 presents the dimensionless radial deflection and force quantities at $x = L/2$, $s = 0$ corresponding to bending moments M_s and M_x as well as membrane forces N_s and N_x. The results presented by Kempner [15] are compared with ones generated using the ASM and the finite-element method (FEM) solution generated using SAP2000. The results of all three methods are in very good agreement.

Table 5. Dimensionless deflection and forces at $x = L/2$ and $s = 0$ for the cylindrical shell subjected to a line load with total magnitude of $P^* = 2c_2p$ in Figure 5.

Method	$\dfrac{wER}{P^*}$	$\dfrac{M_s}{P^*}$	$\dfrac{M_x}{P^*}$	$-\dfrac{N_sR}{P^*}$	$-\dfrac{N_xR}{P^*}$
Kempner (1955)	6211	0.196	0.107	8.094	9.275
ASM	6201	0.190	0.102	8.031	9.304
FEM	6208	0.196	0.105	8.170	9.337

6.4 Example 3: Stiffened Tank

The steel tank in Fig. 6 has a fixed base and is stiffened with standard W10x49 steel rolled sections having an area A = 9290 mm^2 (14.4 in^2) and a moment of inertia I_x = 1.132x10^8 mm^4 (272 in^4). The dimensions and fluid properties for the tank are presented in Table 6. The modulus of elasticity of the tank and stiffener E = 2x10^{8}kPa (29x10^6 psi) and Poisson's ratio v = 0.3.
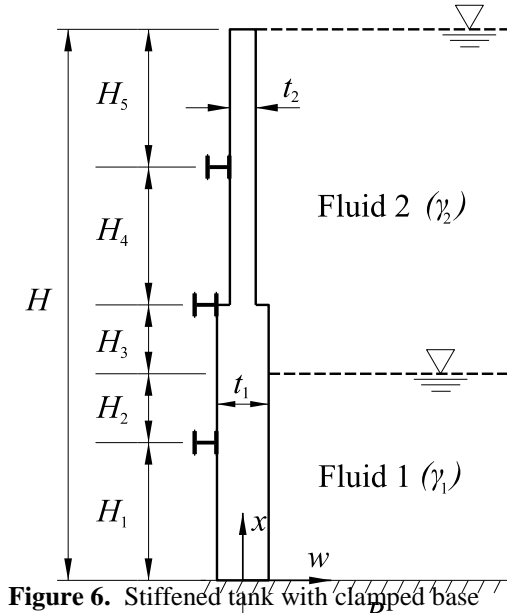
Table 6. Dimensions and fluid properties for the tank in Figure 6

Specific Gravity	γ_1 =	9.81 kN/m^3 (62.4 pcf)
	γ_2 =	7.35 kN/m^3 (46.8 pcf)
Wall Thickness	t_1 =	76.2 mm (3.0 in)
	t_2 =	38.1 mm (1.5 in)
Radius	R =	6.1 m (20 ft)
Height	H =	6.08 m (20 ft)
	H_1 =	1.52 m (5.0 ft)
	H_2 =	0.76 m (2.5 ft)
	H_3 =	0.76 m (2.5 ft)
	H_4 =	1.52 m (5.0 ft)
	H_5 =	1.52 m (5.0 ft)

Figure 6. Stiffened tank with clamped base

The inclusion of the stiffeners and variation in wall thickness and loading through the height of the cylinder limits the use of existing analytical solutions. The Analytical Strip Method (ASM) is deployed by identifying six geometric and loading discontinuities, dividing the cylinder into five strips between the discontinuity points, and imposing boundary and continuity conditions at the ends of each strip. Fig. 7 through Fig. 9 present the radial displacement w, bending moment M_x, and shear Q_x, along the height of the stiffened tank. Comparison with existing analytic methods of solution is not possible. Consequently, the results of the ASM are compared with the finite-element (FEM) results generated using SAP2000. The two results are in good agreement.
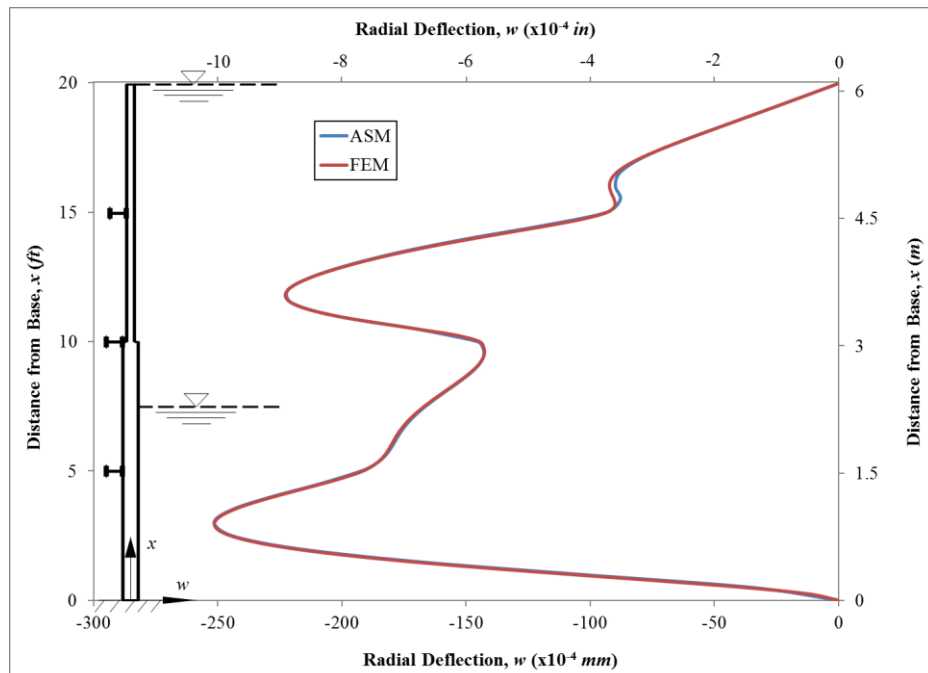
Figure 7. Radial deflection for the stiffened tank in Fig. 6

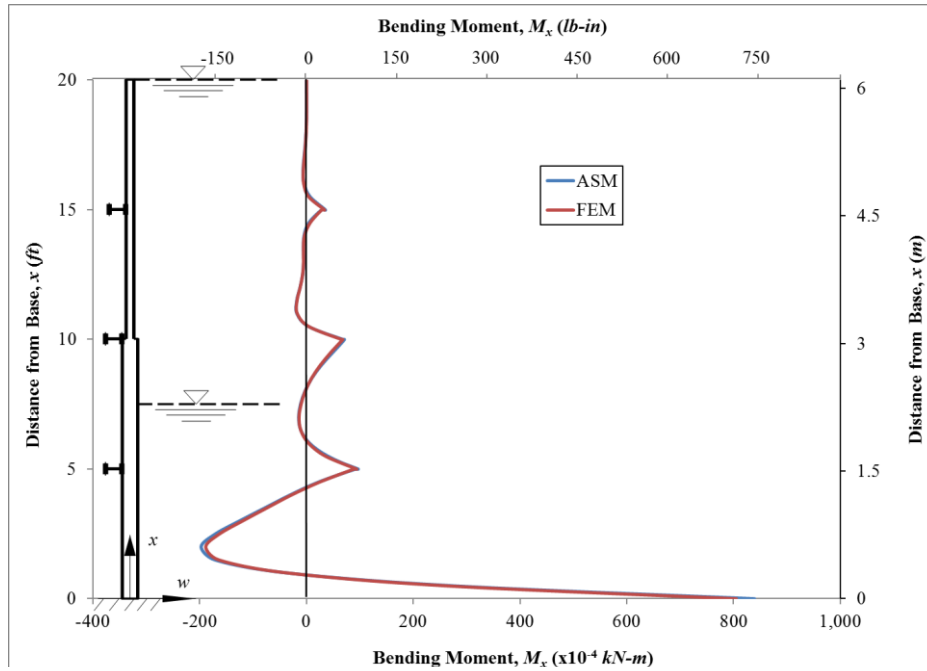*Note: The ASM and FEM results are in very good agreement and difficult to discern in the figure*

Figure 8. Bending moment, M_x, for the stiffened tank in Fig. 6
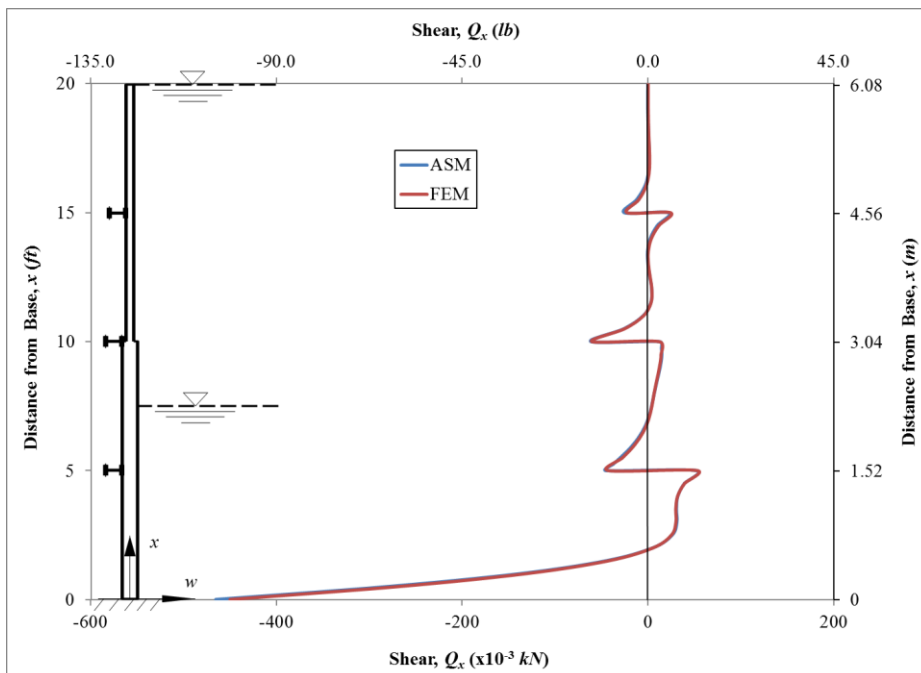*Note: The ASM and FEM results are in very good agreement and difficult to discern in the figure*

Figure 9. Shear, Q_x, for the stiffened tank in Fig. 6
Note: The ASM and FEM results are in very good agreement and difficult to discern in the figure

6.5 Example 4: Stiffened Tank Subjected to Line Load

The purpose of this example is to demonstrate the application of the Analytical Strip Method (ASM) to a stiffened cylinder subjected to non-axisymmetric loading. Existing analytical solutions to these type problems are not available.

The steel cylinder in Fig. 10 is stiffened with standard W10x49 steel rolled sections having an area $A = 9290$ mm^2 (14.4 in^2), a moment of inertia about the section x-axis $I_x = 1.132 \times 10^8$ mm^4 (272 in^4), a moment of inertia about the section y-axis $I_y = 3.888 \times 10^7$ mm^4 (93.4 in^4), and a torsion constant $J = 5.786 \times 10^5$ mm^4 (1.39 in^4). The modulus of elasticity of the cylinder and stiffener $E = 2 \times 10^8$ kPa (29x10^6 psi) and Poisson's ratio $v = 0.3$. The ends are simply supported with boundary conditions, $u = s = w = M_x = 0$. The cylinder is subjected to a line load $p = 0.01$ kN/mm (57.1 lb/in).
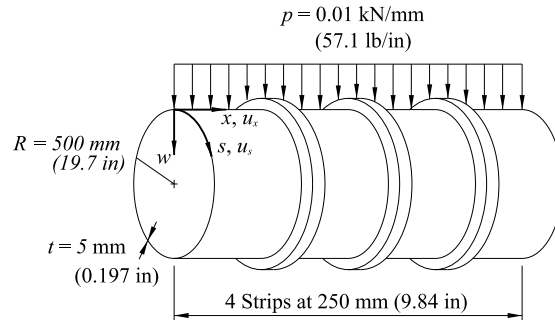

Figure 10. Stiffened cylindrical shell subjected to a line load

The inclusion of the stiffeners, as well as the non-axisymmetric loading, limits the use of analytical solutions. Just as in Example 3, for a shell subjected to axisymmetric loads, the ASM is deployed by identifying four strips between the stiffeners and imposing the boundary and continuity conditions at the ends of each strip. Comparison with existing analytic methods of solution is not possible. Consequently, the results of the ASM are compared with the finite-element (FEM) results generated using SAP2000. Fig. 11 presents the radial deflection along the generator, $s = 0$. There is excellent agreement between the ASM solution and the FEM solution.

The ASM results are based on summation of the first 51 modes. The series shows good convergence characteristics, mode 50 contributes less than 0.04% to the cumulative deflection at $x = 375$ mm (14.8 in) and $x = 500$ mm (19.7 in).
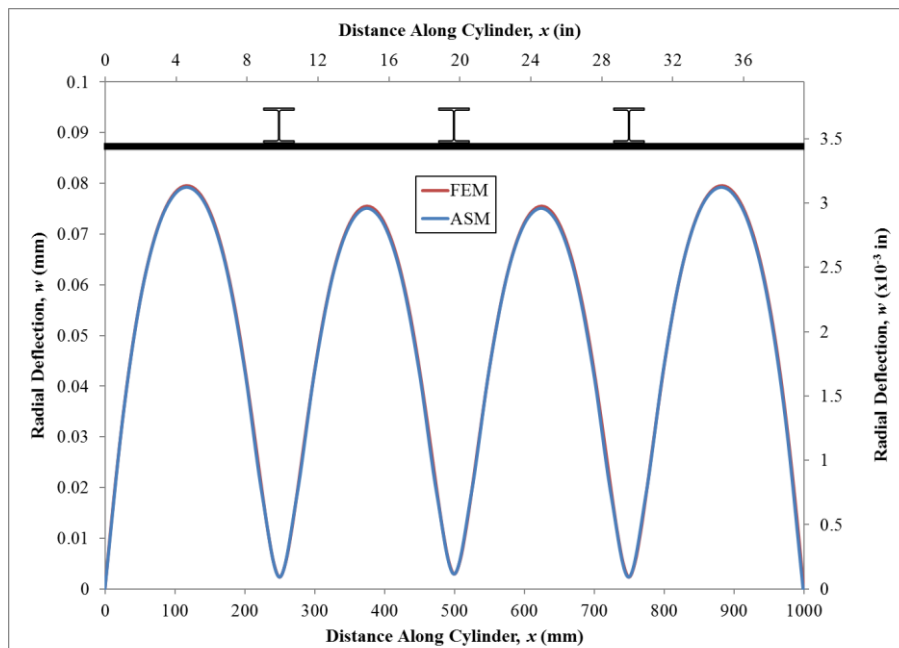

Figure 11. Radial deflection, *w*, along the generator ($s = 0$) for the stiffened cylinder in Fig. 10
Note: The ASM and FEM results are in very good agreement and difficult to discern in the figure

VII.   Conclusions

The Analytical Strip Method (ASM) is presented in this paper for stiffened isotropic cylindrical shells. The primary advantage of the ASM is its applicability to any generalized distribution of ring stiffeners along the length of the shell and to any combination of patch, uniform, line, concentrated, and hydrostatic loads. The following are deduced from the derivation of the ASM and the examples presented in this paper:

- The results of the ASM are in good agreement with existing analytical solutions, and the generality of the solution method overcomes many limitations of existing analytical solutions.
- Unlike the finite element method, the ASM does not require significant pre-processing effort. Its accuracy is dependent on the number of modes considered in the solution rather than the fineness of the discretization of the structure.

- The finite element method does offer more flexibility in structure geometry. For instance, the ASM requires stiffeners to be concentric with the shell walls and stepped wall thicknesses to have a coincident middle surface.
- The finite element method has less potential for numerical instabilities than the ASM.

References

[1]. H. Kraus,*Thin elastic shells* (New York, NY: John Wiley & Sons, Inc., 1967).

[2]. A. Leissa, *Vibration of shells*,NASA SP 288, 1973.

[3]. S. Timoshenko and S. Woinowsky-Krieger,*Theory of plates and shells, 2ⁿᵈ ed.*(York, Pa: McGraw-Hill Book Company, Inc, 1959).

[4]. P. Bijlaard, Stresses from local loadings in cylindrical pressure vessels, *Trans. Am. Soc. Mech. Engrs 77*, 1955, 805-814.

[5]. F. Odqvist, Action of forces and moments symmetrically distributed along a generatrix of thin cylindrical shell, *Trans. Am. Soc. Mech. Engrs 68A*, 1946, 106-108.

[6]. N. J. Hoff, J. Kempner, and F. V. Pohle, Line load applied along generators of thin-walled circular cylindrical shells of finite length, *Quarterly of Applied Mathematics*, *11*, 1954, 411-425.

[7]. R. M. Cooper, Cylindrical shells under line load, *Journal of Applied Mechanics*, *24*, 1957, 553-558.

[8]. A. K. Naghdi, Bendingof a simply supported circular cylindrical shell subjected to uniform line load along a generator, *Int. J. Solids Structures*, *4*, 1968, 1067-1080.

[9]. H.R. Meck, Bending of a thin cylindrical shell subjected to a line load around a circumference, *Journal of Applied Mechanics*, *28*, 1961, 427-433.

[10]. I. E. Harik and G. L. Salamoun, Analytical strip solution to rectangular plates, *Journal of Engineering Mechanics*, *112(1)*, 1986, 105-118.

[11]. I. E. Harik and G. L. Salamoun, The analytical strip method of solution for stiffened rectangular plates, *Computers & Structures*, *29(2)*, 1988, 283-291.

[12]. S. Sharma, N. G. R. Iyengar, and P. N. Murthy, Buckling of antisymmetric cross- and angle-ply laminated plates, *International Journal of Mechanical Sciences*, *22(10)*, 1980, 607-620.

[13]. V. Z. Vlasov, *Thin-walled elastic beams, 2ⁿᵈ ed.* (Jerusalem: Israel Program for Scientific Translations Ltd, 1961)

[14]. Editing Group of the Manual of Mathematics, Roots for quartic equation,*Manual of Mathematics*, (Beijing, China: People's Education Press, 1979) 87-90.

[15]. J. Kempner, Remarks on Donnell's equations, *Journal of Applied Mechanics*, *22*, 1955, 117-118.